Ukrainian Journal of Physical Optics
ISSUE 2
2025

NUMERICAL OPTIMIZATION OF CIGS/CGS DOUBLE-ABSORBER SOLAR CELLS: ENHANCING EFFICIENCY THROUGH THICKNESS AND BANDGAP TUNING

A. NASSOUR[1], M. KANDOUCI[1], Z. ABU WAAR[2], A. BELGHACHI[3], M. MOUSTAFA[4,*]

[1] Department of Electronics, Laboratory of Electronic Photonic and Optronic (LEPO), Djillali Liabes University of Sidi Bel-Abbes, 22000, Algeria
[2] Department of Physics, College of Science, The University of Jordan, Amman, 11942, Jordan
[3] Department of Physics, Laboratory of Physics of Semiconductors Devices (LPDS), Tahri Mohamed University of Béchar, 08000, Algeria
[4] Department of Physics, School of Sciences and Engineering, The American University in Cairo, New Cairo, 11835, Egypt
*Corresponding author: mohamed.orabi@aucegypt.edu

Received: 07.03.2025

Abstract. In this study, we utilized SCAPS simulation to evaluate the performance of an innovative copper indium gallium selenide (CIGS) - based solar cell architecture meticulously designed to achieve superior conversion efficiency. We employed a novel functionality to predict the absorber layer's bandgap and electron affinity across varying gallium (Ga) concentrations (x). To mitigate back-contact recombination losses, we investigated the incorporation of a copper gallium selenide (CGS) layer with a high bandgap (1.7 eV) near the molybdenum back contact, which acts as an electron reflector. The performance enhancement of CIGS solar cells through Ga grading of the absorber layer is demonstrated. Our findings revealed that in a dual-absorber layer configuration, conversion efficiency steadily increased as the CGS layer's thickness approached approximately 90% of the overall absorber thickness. Additionally, we examined the impact of a graded bandgap toward the back of the top absorber layer, i.e., the CIGS. The results demonstrated that an optimized CIGS (graded)/CGS/Mo system exhibits exceptional photovoltaic performance, achieving an optimal efficiency of 25.98%.

Keywords: CIGS solar cells, graded band gap, conversion efficiency, SCAPS simulation

UDC: 535.2, 620
DOI: 10.3116/16091833/Ukr.J.Phys.Opt.2025.02104

1. Introduction

Chalcopyrite-type compound semiconductors with the formula $Cu(In_xGa_{1-x})Se_2$ hold significant promise as absorber materials for thin-film solar cells. These materials are strong contenders for high-efficiency, cost-effective solar technologies and exhibit prime optical and electronic properties, including an enhanced absorption coefficient ($\alpha \sim 10^5$ cm^{-1}) [1]. Thin-film solar cells based on copper–indium–gallium–diselenide (CIGS) have demonstrated efficiencies of ~19.5% [2]. A record efficiency of 17.4% was achieved for a CIGS thin-film sub-module [3], while laboratory-scale devices have reached remarkable efficiency levels of up to 23.6% [4].

These absorber layers typically exhibit an off-stoichiometric composition characterized by the Ga/(Ga+In) ratio (x) [5]. By intermixing $CuInSe_2$ (CISe) and $CuGaSe_2$ (CGSe), the optical bandgap can be engineered within 1.06 eV and 1.7 eV. This ability to customize the absorber bandgap to align with the solar spectrum provides an effective strategy for enhancing solar cell performance. The change in the absorber layer bandgap is directly tied

to changes in its electron affinity (χ) and optical absorption characteristics. The optical absorption coefficient of CIGS at various Ga/(Ga+In) ratios is modeled using the Gloeckler approach [6], enabling the implementation of the so-called Ga-grading. The Ga fraction significantly impacts the electron affinity of CIGS, influencing the conduction band minimum (E_C), while the valence band maximum (E_v) remains largely unaffected by changes in χ [7]. Bandgap engineering can be achieved through two primary approaches: modifying the bandgap near the buffer layer (front grading) or adjusting it towards the back contact of the absorber (back grading). A combination of these methods, known as double grading, involves a gradual decrease in Ga content from the front surface to a minimum point within the absorber (typically near the center) followed by an increase towards the back contact [8, 9]. This double-grading strategy improves carrier collection efficiency and minimizes recombination losses, enhancing the overall performance of the solar cell. Numerous CIGS-based solar cells featuring both standard and double Ga-grading have been developed in recent years; however, the precise impact of this bandgap variation remains uncertain.

A double-graded bandgap profile offers enhanced solar cell performance by simultaneously addressing key parameters. Indeed, front grading enhances the open-circuit voltage (Voc) by optimizing the energy alignment, while back grading facilitates the efficient collection of photogenerated carriers, thereby increasing the photocurrent (J_{sc}) [10]. The optimal bandgap at the back contact plays a critical role in achieving the desired increase in J_{sc} [11]. Song et al. [12] modeled a CGS/CIGS tandem solar cell. They demonstrated that a conversion efficiency of 25% is attainable when a high-efficiency CGS at the top is paired with an optimized CIGS as a bottom cell. Furthermore, simulation studies using SCAPS for CIGS double-absorber solar cells have reported a best-achieved efficiency of 22.32%, highlighting the potential of this configuration for high-performance photovoltaic applications [13].

To optimize the high performance of the CIGS-based solar cells with low-cost semiconductor material and fabrication process, it is necessary to investigate and develop alternative designs of the absorber constituents and to obtain more details in understanding their properties for different structure layers. Recently, a high conversion efficiency of 45.23% was achieved by optimizing a double junction CGS/CIGS solar cell under current matching conditions using SILVACO software [14]. The literature mentions that single-junction solar cells have limited efficiency. On this basis, we propose a single-junction architecture with a double absorber CGS/CIGS solar cell as another option to reduce the recombination rate in this conventional structure and improve the performance of thin-film solar cells.

This paper aims to investigate factors limiting the performance of modern graded CIGS solar cells using the SCAPS-1D simulation package [15, 16]. The study examines two types of solar cell designs. The first involves a single absorber layer of CIGS, where the influence of parameters such as absorber thickness and bandgap on photovoltaic performance is systematically analyzed. The second one features a bi-layer structure with a CIGS/CGS absorber. A numerical analysis was performed to assess the effect of integrating a CGS layer near the molybdenum back contact on the performance of CIGS solar cells. A parameter, r_{CGS}, is introduced to represent the ratio of the CGS layer thickness (d_1) to the total absorber thickness (d), with r_{CGS} values ranging from 0.1 to 0.9. The study further explores the benefits of a linear back-graded CIGS top absorber on device efficiency, considering a spatially linear bandgap variation and optimizing the grading profile [1].

2. Device configuration and simulation methodology

Numerical modeling is crucial in understanding and interpreting experimental results for CIGS-based solar cells while evaluating the potential advantages of different cell structures. Various software tools, including SCAPS-1D [15, 16], PC-1D [17], AFORS-HET [18], AMPS-1D [19], and ASA [20], have been initiated to simulate the performance of multilayer thin-film solar cells. In this study, we extensively utilized SCAPS-1D to investigate and optimize device performance. The simulations were conducted under an AM 1.5 light spectrum with P=1000 W/m^2 and at a room temperature T=300 K. The baseline solar cell configuration considered is a ZnO: Al/ZnO/CdS/CIGS/Mo/substrate structure, as illustrated in Fig. 1a. The key component of this photovoltaic device is the CIGS absorber layer, which was initially modeled as a single-layer absorber akin to conventional CIGS solar cells. Subsequently, we explored an innovative bi-layer absorber structure of CIGS/CGS, shown in Fig. 1b, to investigate its potential for enhanced performance.

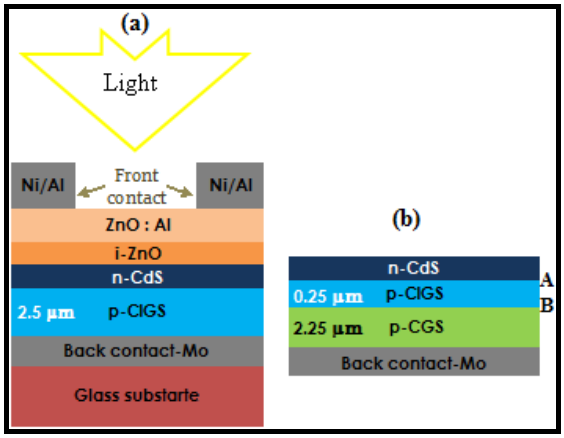

Fig. 1. (a) Single absorber layer CIGS solar cell structure. (b) Bi-layer cell CIGS/CGS. The bottom layer is CGS (1.7 eV), and the top is CIGS (1.26 eV).

The parameters of the different layers, bulk defect properties, and contact parameters extracted from reported literature [21-25] are displayed in Table 1. The material properties of the buffer and window layers are held constant throughout the simulation. The band gap of the absorber increases from 1.06 eV (pure CISe) to 1.7 eV (pure CGSe), and electron affinity ranges from 4.6 eV to 3.41 eV, according to the following equations [7]:

$$E_g(x) = 1.06(1-x) + 1.7x - 0.24762x(1-x), \quad (1)$$

$$\chi(x) = 4.6(1-x) + 3.41x - 0.03333x(1-x). \quad (2)$$

The term (1-x) coefficients represent the band gap and electron affinity of the ternary compound CISe, while the coefficients of the (x) term are E_g and χ of the ternary compound CGSe. Moreover, the third coefficient is the bowing parameter representing non-linear components' amplitude.

First, We have chosen donors and acceptors concentrations to equal N_D=1×10^{17} cm^{-3} and N_A= 2×10^{16} cm^{-3} [6], respectively. A single deep acceptor and donor defect type were used for the CdS and CIGS layers, respectively. The CdS and ZnO layers are characterized by a high defect density comparable to the shallow donor density, contributing to the commonly observed photoconductivity [25]. When surface states are absent, the majority carrier barrier height for holes can be expressed as follows [26]

$$\Phi_B = E_g + \chi - \Phi_m \quad (3)$$

Table 1. The parameters of the input layer, defect and contact properties for the simulation of CIGS solar cells.

Parameters	**CIGS**	**CdS**	**ZnO**	**ZnO:Al**
Thickness (d), μm	Variable	0.05	0.2	0.2
Bandgap (E_g), eV	Variable	2.4	3.3	3.3
Electron affinity (χ), eV	Variable	4.2	4.4	4.4
Dielectricrelative permittivity (ε_r)	13.6	10	9	9
Density of states (N_c) in conduction band (C_B), cm^{-3}	2.2×10^{18}	22×10^{18}	2.2×10^{18}	2.2×10^{18}
Density of states (N_v) in valence band (V_B), cm^{-3}	1.8×10^{19}	1.8×10^{19}	1.8×10^{19}	1.8×10^{19}
Electron mobility (μ_e), cm^2/V s	100	100	100	100
Hole mobility (μ_h), cm^2/V s	25	25	25	25
Donor density (N_D), cm^{-3}	0	10^{17}	10^{18}	10^{20}
Acceptor density (N_A), cm^{-3}	2×10^{16}	0	0	0
Defect properties				
Capture cross-section electrons (σ_e), cm^2	5×10^{-13}	10^{-17}	10^{-12}	10^{-12}
Capture cross-section holes (σ_h), cm^2	10^{-15}	10^{-12}	10^{-15}	10^{-15}
Defect density (N), cm^{-3}	10^{14}	10^{18}	10^{17}	10^{17}
Contact parameters	**Back Contact**		**Front Contact**	
Recombination velocity for electron (S_e), cm/s	10^7		10^7	
Recombination velocity for holes (S_h), cm/s	10^7		10^7	
Reflectance	0.8		0.05	
back contact barrier (Φ_B), eV	Variable		0	

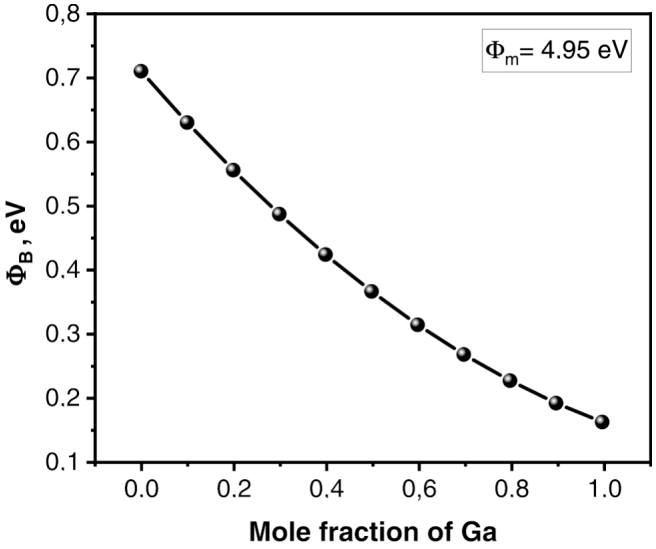

Fig. 2. Variation of back contact barrier Φ_B due to the increase of Ga content in CIGS composition for Φ_m = 4.95 eV. The values of Φ_B are calculated by Eq. (3) while E_g and χ are varied as a function of Ga mole fraction by Eqs. (1) and (2).

Fig. 2 shows the variation of Φ_B at different Ga/(Ga+In) ratios for a metal work function Φ_m Mo=4.95 eV. This back contact barrier decreases almost linearly by increasing Ga content in $CuIn_{1-x}Ga_xSe_2$.

3. Results and discussion

3.1. The effect of absorber layer thickness and band gap on CIGS cell performance

The effect of absorber layer thickness on cell performance was simulated across a range from 0.2 μm to 3 μm, considering both low and optimal absorber layer band gaps, as discussed in Ref. [26]. The simulations were conducted at various energy gap values determined as functions of composition (x) from Eq. (1) while maintaining all other material parameters unchanged and varying the absorber thickness, as shown in Fig. 3. The results indicate that increasing the thickness from 0.2 μm to 2.5 μm enhances efficiency values. Notably, the efficiency remains nearly constant for absorber thicknesses greater than 1 μm, specifically in the range of 1 μm<d<3 μm. These simulations identified an optimum thickness of 2.5 μm, independent of the energy gap. This finding aligns well with previously reported results in Refs. [27, 28].

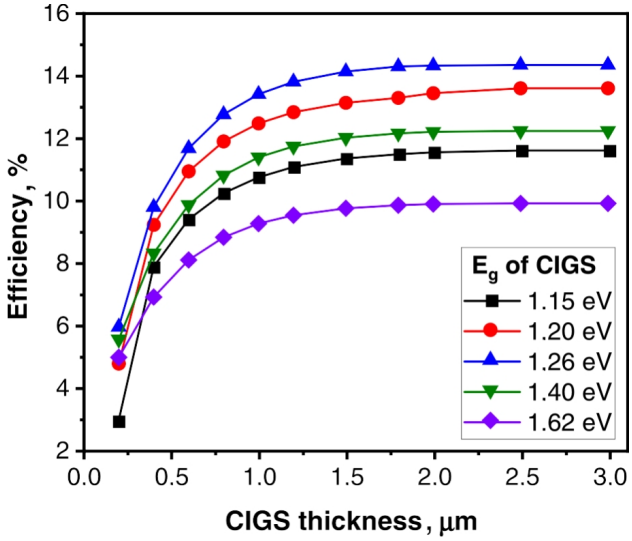

Fig. 3. Baseline CIGS solar cell efficiency versus CIGS absorber thickness at varying absorber energy gap values.

Fig. 4 illustrates the variation in quantum efficiency (QE) of baseline CIGS solar cell as a function of incident light wavelength at different CIGS thicknesses. For thicknesses greater than 0.5 μm, the collection efficiency of photo-generated carriers improves, and complete photon absorption is achieved with increasing layer thickness. This enhancement is attributed to a reduction in the junction depth. It is well established that recombination is primarily influenced by the junction depth, as discussed in Ref. [29]. For a d=2.5 μm thickness, more photons are absorbed due to the increased optical path length, allowing for greater interaction between the incident light and the absorber material. This enhanced photon absorption results in more photogenerated charge carriers, improving performance. The calculation of short-circuit current density(J_{sc}), open-circuit voltage (V_{oc}), fill factor (FF), and conversion efficiency (η) values for various energy gap ranges is shown in Table 2, with the efficiency curve versus energy gap presented in Fig. 5. The absorber's band gap and electron affinity are adjusted according to the Ga content, as per Eq. (1) and (2). The results indicate that efficiency peaks at an energy gap of approximately 1.26 eV, corresponding to a Ga/(Ga+In) ratio of 0.4. This finding aligns with previous studies reported in Ref. [9]. Beyond this point, efficiency decreases with a wider band gap in the CIGS absorber layer.

Table 2. Comparative table of the cell performance as a function of the CIGS absorber bandgap.

E_g,eV	V_{oc},V	J_{sc}, mA/cm^2	FF, %	η, %
1.15	0.588	28.721	76.34	11.64
1.2	0.676	27.674	75.5	13.65
1.26	0.742	26.443	74.85	14.35
1.32	0.801	25.166	66.37	13.37
1.4	0.87	23.498	48.49	12.23
1.48	0.89	22.22	46.94	10.55
1.55	0.947	21.566	46.07	10.04
1.62	0.982	20.32	46.03	9.9

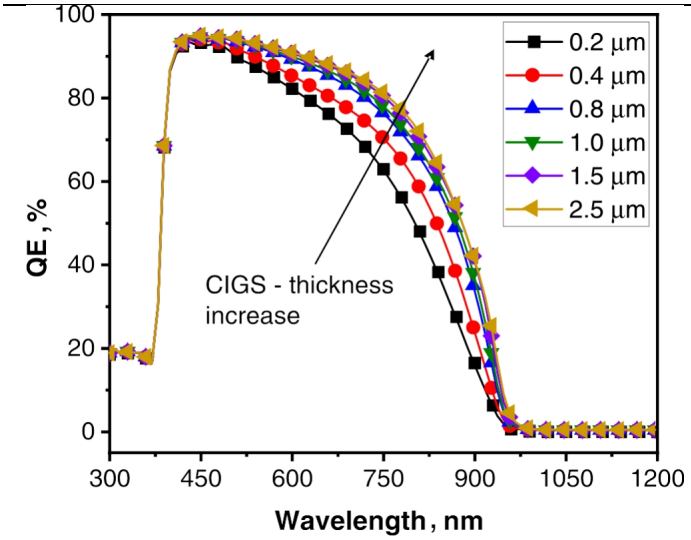

Fig. 4. Quantum efficiency of the cell as a function of incident light wavelength when the thickness of the absorber layer increases.

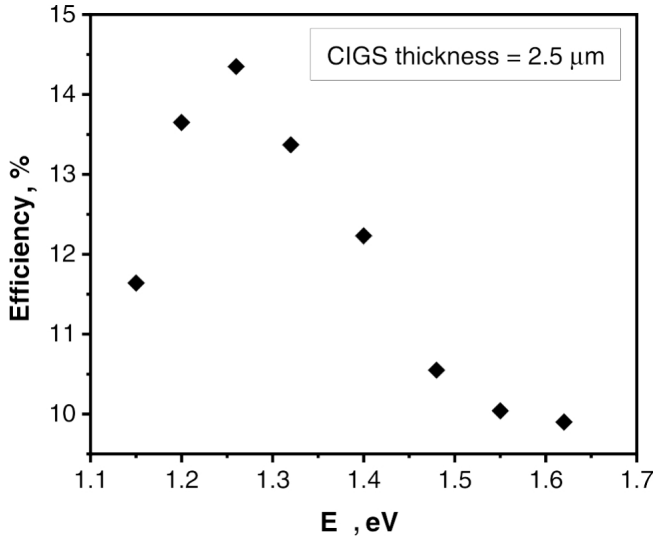

Fig. 5. Variation of baseline CIGS solar cell efficiency as a function of CIGS energy band gap for a 2.5 µm thick absorber layer.

The same trend is observed for other thickness values, with the maximum *FF* of about 75% achieved for a uniform band gap of 1.26 eV, which correlates with the lowest defect density. Further increases in the band gap by adding gallium do not provide additional benefits and can adversely affect the solar cell's performance. Experimentally, enhancing the band gap (E_g) by increasing gallium content is not an ideal solution, as it introduces defects in regions with high Ga content, as reported in Refs. [30, 31]. Consequently, as the Ga/(Ga+In) ratio rises, the carrier concentration increases, reducing the depletion region width. This effect is demonstrated in Fig. 6, where the space charge region thickness is plotted versus voltage for lower (x = 0.2) and higher (x = 0.8) Ga mole fractions. As seen, CIGS cells with higher Ga content exhibit a higher recombination rate, further diminishing their efficiency.

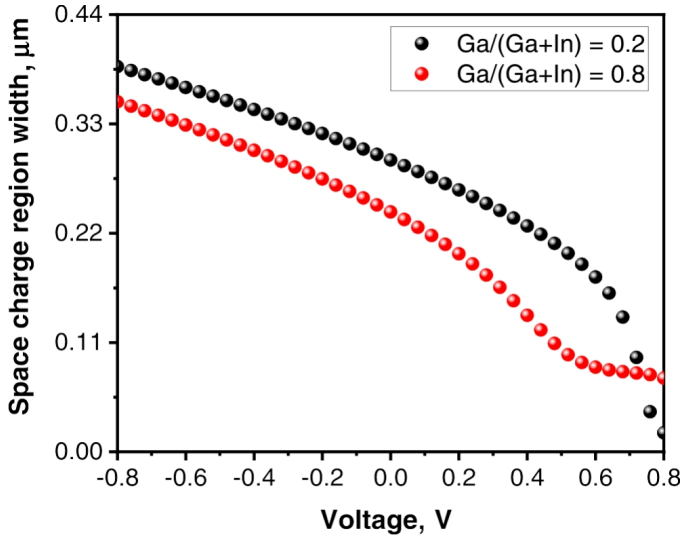

Fig. 6. The thickness of space charge region versus voltage for lower (x = 0.2) and high (x = 0.8) Ga content.

3.2. The introduction of a CGS double absorber layer in the back contact

Alternative cell structures with a variable absorber composition have been explored in the literature to address this limitation, particularly with an increased energy gap near the Mo back-contact region [32]. Introducing a Ga-rich layer at the CIGS/Mo interface maintains high conductivity for the majority holes while simultaneously reflecting minority electrons. Adding the CGS layer helps repel electrons away from the Mo contact, preventing their capture and thus enhancing the J_{sc} [27]. Consequently, we optimize this novel structure by placing a CIGS layer on top of the CGS bottom layer, as illustrated in Fig. 1b.

In this study, the CIGS layer near the junction has a Ga fraction of x = 0.4 (E_g = 1.26 eV), corresponding to the optimal cell configuration. All parameters of the layers are kept constant, except for the Ga/(Ga + In) ratio and the thickness of the bottom layer near the Mo back contact. The top layers, ZnO and CdS, remain unchanged. Fig. 7 illustrates the variation in efficiency as a function of the Ga/(Ga+In) ratio in the bottom absorber layer of $CuIn_{0.6}Ga_{0.4}Se_2/CuIn_{1-x}Ga_xSe_2/Mo$, with varying r_{CGS} values from 10% to 90%. Here, r_{CGS} represents the ratio of the bottom absorber layer thickness to the total thickness of the single absorber layer (2.5 µm).

The addition of Ga content has a positive effect on the solar cell's performance. For a high Ga content (x = 1), the efficiency reaches a maximum value of 17.4%, corresponding to a 90% thick $CuGaSe_2$ bottom layer and 10% of $CuIn_{0.6}Ga_{0.4}Se_2$ as the top layer. To confirm that the optimum thickness of the CGS bottom layer is 90% of the total absorber thickness (2.5 μm), the efficiency as a function of r_{CGS} is presented in Fig. 8. The two endpoints on this plot depict the efficiencies of a single $CuIn_{0.6}Ga_{0.4}Se_2$ layer (r_{CGS} = 0) and a single $CuGaSe_2$ layer (r_{CGS} = 1). The efficiency increases significantly from 14.35% to 17.4% as r_{CGS} increases from 0 to 0.9, then gradually decreases with further increases in r_{CGS} from 0.9 to 1, with a step of 0.01 (inset of Fig. 8).

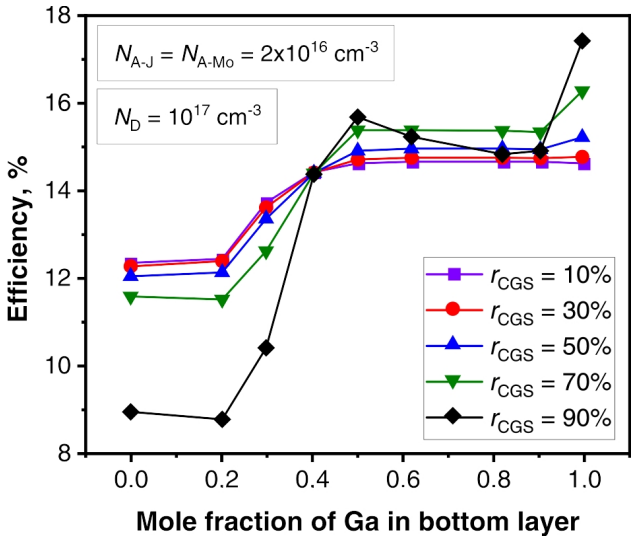

Fig. 7. Dependence of efficiency on the mole fraction of Ga in the bottom absorber layer of $CuIn_{0.6}Ga_{0.4}Se_2/CuIn_{1-x}Ga_xSe_2$ for various ratios (r_{CGS}) of the bottom absorber layer to the total thickness of the absorber layer (2.5 μm). N_{A-J} and N_{A-Mo} represent the acceptor densities near the junction and back contact, respectively.

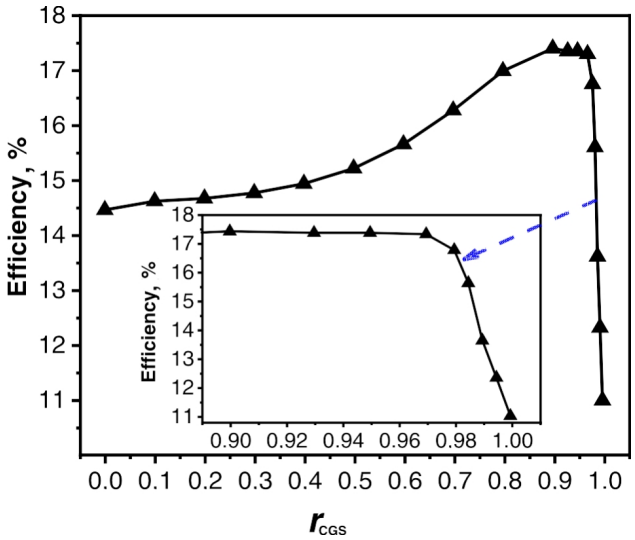

Fig. 8. Efficiency values versus ratios (r_{CGS}) of the CGS bottom absorber layer to the total thickness of the absorber layer (2.5 μm). The inset shows magnifications of r_{CGS} from 0.9 to 1.

Table 3. Optimized photovoltaic parameters of single and double absorber layers.

Absorber layer	V_{oc}, V	J_{sc}, mA/cm^2	FF, %	H, %
CIGS	0.742	26.443	74.85	14.35
CIGS/CGS	0.804	28.910	76.65	17.4

The comparison between the performance of a single-layer cell and its bi-layer counterpart is noteworthy. For a 2.5 μm thick cell, the bi-layer structure consisting of a 0.25 μm thick $CuIn_{0.6}Ga_{0.4}Se_2$ (E_g = 1.26 eV) layer on top of a 2.25 μm thick CGS (E_g = 1.7 eV) layer outperforms its single-layer CIGS counterpart (E_g = 1.26 eV). The efficiency of the CIGS/CGS bi-layer cell reached 17.4%, while the corresponding value for the single-layer CIGS cell with x = 0.4 was 14.35%. Table 3 compares the optimized single and double absorber layer cells' photovoltaic parameters. The (J-V) characteristics of both the bi-layer and single-layer cells are shown in Fig. 9. From this graph, it is evident that both the J_{sc} and open V_{oc} improve in the optimized bi-layer structure, with an increase of 2.5 mA/cm^2 for J_{sc} and 62 mV for V_{oc}. A CGS/Mo interface with a Ga mole fraction of 1 provides a minimal back contact barrier of 0.16 eV (as shown in Fig. 2), ensuring high conductivity for majority carriers at the metal-semiconductor interface. This leads to a significant improvement in J_{sc}.

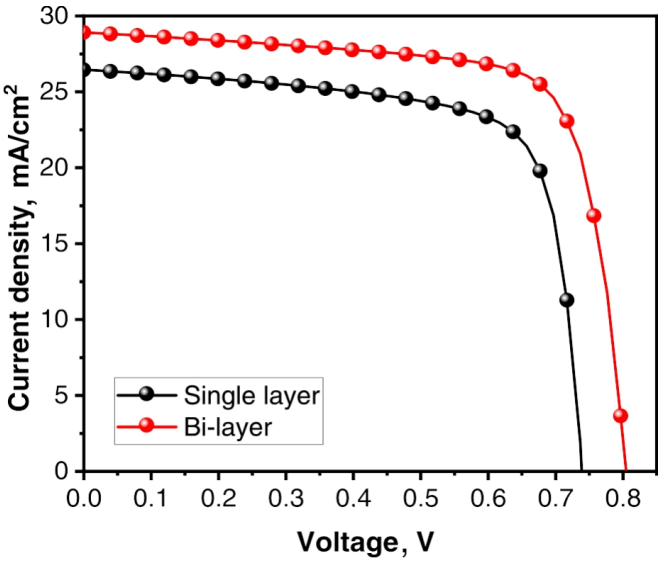

Fig. 9. Comparison between the photocurrent density-voltage (J-V) curves for the single-layer cell (black line) and the bi-layer cell (red line).

The recombination rate (R) can be calculated as an approximation using the following formula [31]:

$$R = \frac{n\,p}{\tau(n+p)}, \tag{4}$$

where τ is the minority lifetime; n and p are the electron and hole concentration, respectively. In the back contact part of the CGS bottom layer and under low injection (low absorption due to large band gap), we have $n << p$. The Shockley-Read-Hall recombination of Eq. (4) reduces to:

$$R = n/\tau \tag{5}$$

This indicates that the total recombination is primarily governed by the excess concentration of minority electrons. The profiles of minority carrier densities (in this case, electrons) for the optimized bi-layer and single-layer cells are shown in Fig. 10. It is evident that the electron density at the Mo/CGS interface (in the double absorber layer structure) is significantly reduced, as is the case at the Mo/CIGS interface (in the single absorber layer structure).

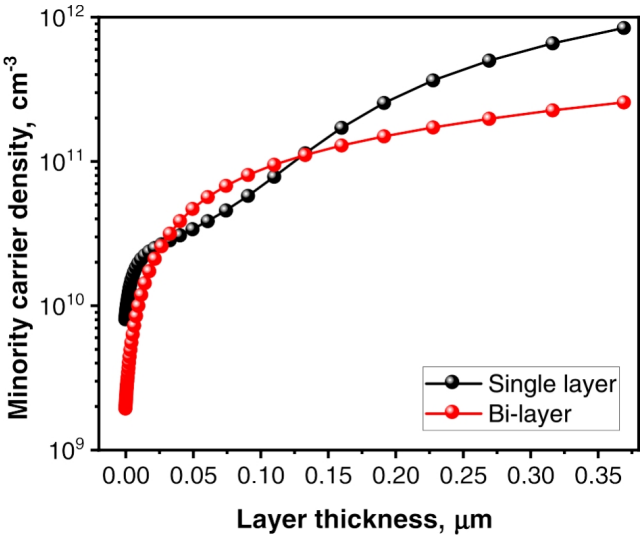

Fig. 10. Simulated minority carrier density profile at the CIGS/Mo and CGS/Mo interface for single-layer absorber and bi-layer (CGS bottom layer), respectively.

This reduction suggests the accumulation of majority carriers (holes), which creates an energy barrier that prevents minority carriers from recombining. The accumulation of positive charges generates an internal electric field that repels minority carriers away from the trap-rich CGS/Mo interface, thereby reducing the recombination rate, as depicted in Fig. 11. This Fig shows the recombination rate profiles at the back contact interface for both the optimized single absorber layer and bi-layer structures, providing a clear explanation for the observed performance enhancement in the cells.

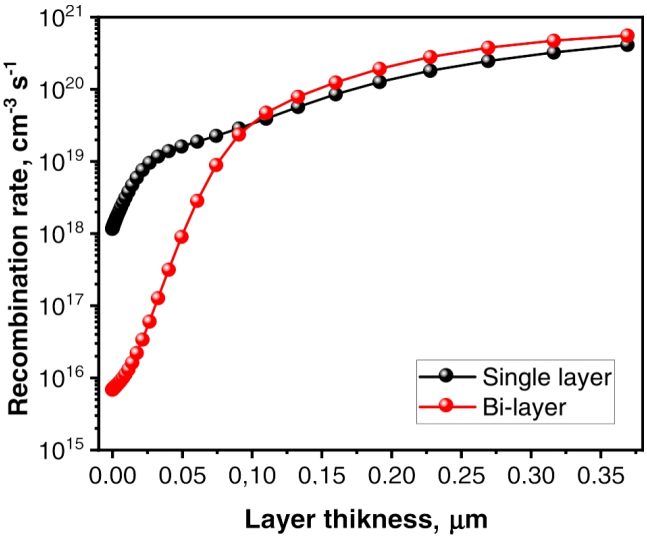

Fig. 11. Simulated recombination rate profile at the CIGS/Mo and CGS/Mo interface for single-layer absorber and bi-layer (CGS bottom layer), respectively.

3.3. The effect of Ga-Grading on CIGS cell performance

A bi-layer structure can be viewed as a simple alternative to a graded junction, widely known to enhance solar cell performance. For example, C. Guillen et al. [32] simulated CIGS solar cells with a graded CIGS layer that exhibits a linear variation towards the back of the device. Kaufmann et al. [28] concluded that most of the performance improvement in these devices is due to the increase in Ga content near the Mo back contact. To investigate the effect of a graded band-gap CIGS absorber in the newly proposed CIGS/CGS bi-layer structure, we adopt a grading model characterized by a linear variation in Ga content (x) throughout the

CIGS top layer. This approach results in two distinct band gaps: one at the front side (A) and one at the back side (B), as shown in Fig. 1b. Our study considers all possible cases, independently varying the Ga ratio at both ends from $x = 0$ to $x = 1$.

This study enables the analysis of different single-grading approaches towards the back of the CIGS top absorber layer. Two distinct effects are induced by fixing the band gap at the CIGS/CGS interface and gradually increasing the front band gap of the CIGS top layer. First, the absorption of photons decreases, with only those possessing higher energies being absorbed, which leads to a drop in the J_{sc}, as shown in Fig. 12. In the same figure, it can be observed that when the front bandgap is fixed, a photo-current increase occurs when the front bandgap is raised below the previously identified uniform band-gap value, as confirmed by A. Belghachi et al. [33]. Second, the increase in the absorption of higher-energy photons increases the V_{oc}, which then saturates at higher values (Eg> 1.53 eV and x> 0.8), as illustrated in Fig. 13. This behavior of V_{oc} has been previously reported by Jo et al. when examining CIGS thin films with varying Ga content, prepared using a co-evaporation technique [34].

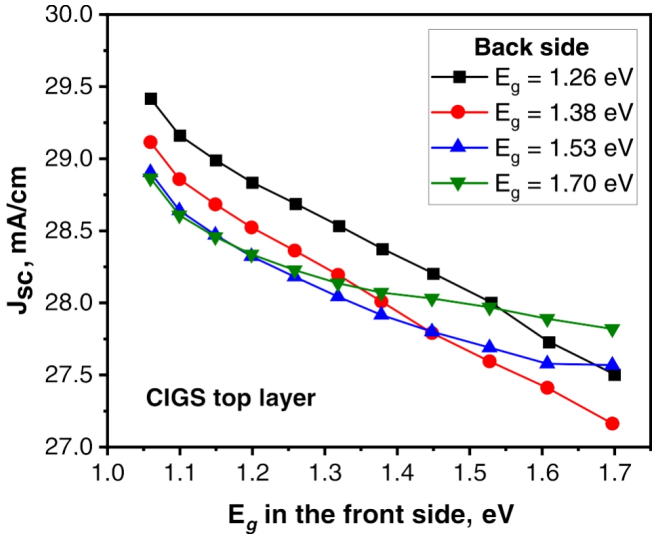

Fig. 12. Short-circuit current density versus the energy band gap at the front of the CIGS top absorber at several different values of E_g at the back of this layer.

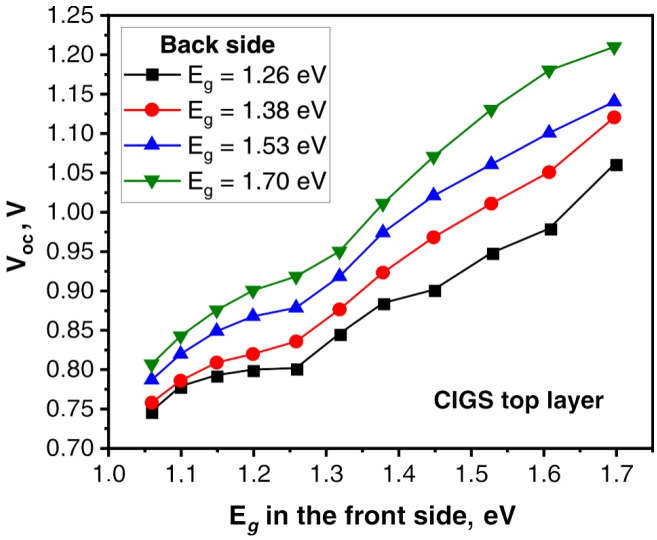

Fig. 13. Open circuit voltage versus the energy band gap at the front of the CIGS top absorber at several different values of E_g at the back of this layer.

The V_{oc} of a solar cell is influenced by the photo-generated current (J_{ph}) and the saturation current (J_0), as expressed in Eq. (6) [35]:

$$V_{oc} = \frac{nkT}{q} \ln\left(\frac{J_{ph}}{J_0} + 1\right), \tag{6}$$

where n is the ideality factor, k and T are the Boltzmann's constant and absolute temperature, respectively. J_{ph} is linked to the generation of electron-hole pairs through the absorption process within the solar cell. Consequently, it can be inferred that the CGS layer beneath the CIGS layer contributes to the absorption process, ultimately enhancing V_{oc}. On the other hand, J_0 is governed by recombination within the solar cell, making V_{oc} an indicator of the recombination level in the device.

Table 4. Comparison of output parameters of the optimized bi-layer structure with previously reported in the literature.

Photovoltaic values	This work CIGS (graded)/CGS	Ref. [12] CGS/CIGS	Ref. [13] CIGS/CIGS	Ref. [33] CIGS (graded)
η, %	25.98	15.3	22.32	24.34
FF, %	85.75	84	78.43	85.02
J_{sc}, mA/cm^{-2}	27.96	14.9	32.45	29.10
V_{oc}, V	1.13	1.2	0.789	0.98

The high V_{oc} and the bandgap saturation threshold can be attributed to the constant defect density assumed in our model. Fig. 14 presents the energy conversion efficiency of a simulated bi-layer structure (CIGS graded/CGS) as a function of the single linear energy band-gap grading at the front of the CIGS top absorber layer, ranging from 1.06 eV to 1.7 eV, corresponding to Ga/(In+Ga) ratios from 0 to 1 (as per Eq. (1)). The maximum efficiency, approximately 25.95%, is achieved with a grading towards the back contact of the CIGS layer with E_g = 1.53 eV (x = 0.8) at the front and E_g = 1.7 eV at the back, located near the junction. It

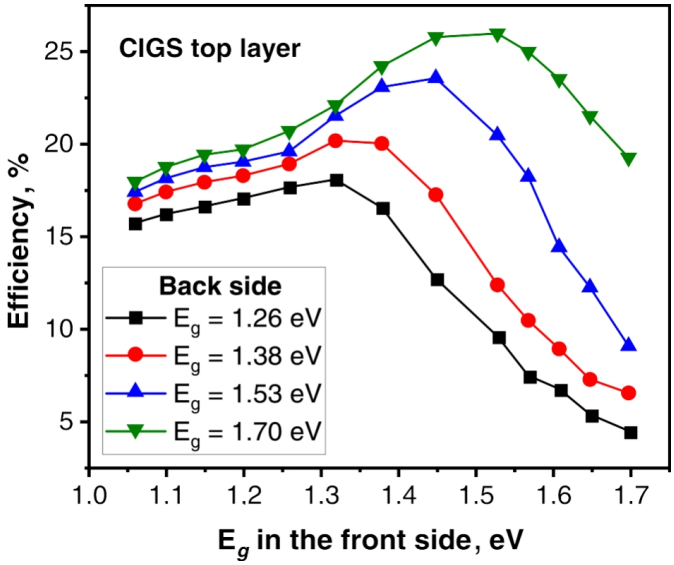

Fig. 14. Efficiency versus the energy band gap at the front of the CIGS top absorber at several different values of E_g at the back of this layer.

is also shown that bulk recombination in the CIGS layer is relatively low in the graded CIGS layer, particularly at the CIGS/CGS interface, when the gap values for both the CGS bottom absorber layer and the back of the CIGS top absorber layer are the same (E_g = 1.7 eV, corresponding to x = 1). The recombination rate at the interface between the back-graded CIGS and CGS is significantly reduced, which explains the observed improvement in cell performance. By incorporating the optimal parameters identified, we have designed the ideal bi-layered CIGS (back-graded)/CGS structure for the solar cell of interest. Our results, which are summarized in Table 4, show improved efficiency compared to previously studied configurations (bi-layered CIGS/CGS and graded CIGS cells), as reported in Refs. [12, 13, 33].

4. Conclusion

In this study, we used the SCAPS-1D simulation tool to investigate the effects of the absorber band gap and thickness on the electrical parameters of single-layer CIGS solar cells. The results indicated that the maximum efficiency is obtained when the band gap is around 1.26 eV. Furthermore, the electrical parameters remained stable when the absorber thickness exceeded 2.5 μm, though the efficiency was relatively low compared to other reported structures.

To improve performance, we optimized a novel bi-layer structure consisting of a CIGS layer on top of a gallium-rich CGS layer at the CGS/Mo interface. The optimal efficiency was achieved when the CGS bottom layer comprised 90% of the total absorber thickness.

Additionally, we examined the effect of a graded band gap in the CIGS layer, with a linear variation of Ga content at the interfaces. Our results showed that a graded band gap, particularly with a higher Ga content at the back of the absorber, significantly reduces recombination at the CIGS/CGS and CGS/Mo interfaces. This resulted in an efficiency of 25.98%.

To further optimize solar cell performance, ongoing research will focus on surface recombination and defect density at the CGS/Mo interface.

Funding. This research received no specific grant from funding agencies in the public, commercial, or not-for-profit sectors.

Acknowledgments. The authors sincerely thank Dr. Marc Burgelman and his colleagues for supplying the SCAPS simulation software.

Disclosures. The authors declare no conflicts of interest.

References

1. Tobbeche, S., Kalache, S., Elbar, M., Kateb, M. N., & Serdouk, M. R. (2019). Improvement of the CIGS solar cell performance: structure based on a ZnS buffer layer. *Optical and Quantum Electronics*, *51*, 1-13.
2. Bhattacharya, R. N., Contreras, M. A., Egaas, B., Noufi, R. N., Kanevce, A., & Sites, J. R. (2006). High efficiency thin-film $CuIn_{1-x}Ga_xSe_2$ photovoltaic cells using a $Cd_{1-x}Zn_xS$ buffer layer. *Applied Physics Letters*, *89*(25).
3. Powalla, M., Jackson, P., Witte, W., Hariskos, D., Paetel, S., Tschamber, C., & Wischmann, W. (2013). High-efficiency $Cu(In,Ga)Se_2$ cells and modules. *Solar Energy Materials and Solar Cells*, *119*, 51-58.
4. Sivasankar, S. M., Amorim, C. O., & da Cunha, A. F. (2025). Progress in thin-film photovoltaics: A review of key strategies to enhance the efficiency of CIGS, CdTe, and CZTSSe solar cells. *Journal of Composites Science*, 9(3), 143.
5. Díaz-Loera, A., Ramos-Serrano, J. R., & Calixto, M. E. (2022). Semiconducting $CuIn(S_x, Se_{1-x})_2$ thin-film solar cells modeling using SCAPS-1D. *MRS Advances*, *7*(2), 28-32.
6. Gloeckler, M., Fahrenbruch, A. L., & Sites, J. R. (2003, May). Numerical modeling of CIGS and CdTe solar cells: setting the baseline. In *3rd World Conference onPhotovoltaic Energy Conversion, 2003. Proceedings of* (Vol. 1, pp. 491-494). IEEE.

7. Khoshsirat, N., Yunus, N. A. M., Hamidon, M. N., Shafie, S., & Amin, N. (2015). Analysis of absorber layer properties effect on CIGS solar cell performance using SCAPS. *Optik*, *126*(7-8), 681-686.
8. Decock, K., Lauwaert, J., & Burgelman, M. (2010). Characterization of graded CIGS solar cells. *Energy Procedia*, *2*(1), 49-54.
9. Parisi, A., Pernice, R., Rocca, V., Curcio, L., Stivala, S., Cino, A. C., Cipriani, G., Di Dio, V., Galluzzo, G.R., Miceli, R. & Busacca, A. C. (2015). Graded carrier concentration absorber profile for high efficiency CIGS solar cells. *International Journal of Photoenergy*, *2015*(1), 410549.
10. Gloeckler, M., & Sites, J. R. (2005). Band-gap grading in Cu(In,Ga)Se_2 solar cells. *Journal of Physics and Chemistry of Solids*, *66*(11), 1891-1894.
11. Mattheis, J., Rostan, P. J., Rau, U., & Werner, J. H. (2007). Carrier collection in Cu(In,Ga)Se_2 solar cells with graded band gaps and transparent ZnO: Al back contacts. *Solar Energy Materials and Solar Cells*, *91*(8), 689-695.
12. Songa, J., Lia, S. S., Huanga, C. H., Andersonb, T. J., & Crisalleb, O. D. Modeling and Simulation of a $CuGaSe_2$/Cu (In_{1-x}, Ga_x)Se_2 tandem solar cell. In *Proceedings of the 3 World Conference on Photovoltaic Energy Conversion Conference. Osaka.*
13. Atourki, L., Kirou, H., Ihlal, A., & Bouabid, K. (2016). Numerical study of thin films CIGS bilayer solar cells using SCAPS. *Materials Today: Proceedings*, *3*(7), 2570-2577.
14. Soheili, A., Hayati, M., & Shama, F. (2020). An optimized efficient double junction CGS/CIGS solar cell with improved performance. *Optik*, *222*, 165461.
15. M. Burgelman, P. Nollet and S. Degrave, 2000. Modelling polycrystalline semiconductor solar cells.Thin Solid Films. **361-362**:527–532.
16. Degrave, S., Burgelman, M., & Nollet, P. (2003, May). Modelling of polycrystalline thin film solar cells: new features in SCAPS version 2.3. In *3rd World Conference onPhotovoltaic Energy Conversion, 2003. Proceedings of* (Vol. 1, pp. 487-490). IEEE.
17. Basore, P. A., & Clugston, D. A. (1996, May). PC1D version 4 for Windows: from analysis to design. In *Conference Record of the Twenty Fifth IEEE Photovoltaic Specialists Conference-1996* (pp. 377-381). IEEE.
18. Singh, S., Kumar, S., & Dwivedi, N. (2012). Band gap optimization of p–i–n layers of a-Si: H by computer aided simulation for development of efficient solar cell. *Solar Energy*, *86*(5), 1470-1476.
19. Hernandez-Como, N., & Morales-Acevedo, A. (2010). Simulation of hetero-junction silicon solar cells with AMPS-1D. *Solar Energy Materials and Solar Cells*, *94*(1), 62-67.
20. Dagamseh, A. M. K., Vet, B., Šutta, P., & Zeman, M. J. S. E. M. (2010). Modelling and optimization of a-Si: H solar cells with ZnO: Al back reflector. *Solar Energy Materials and Solar Cells*, *94*(12), 2119-2123.
21. Benmir, A., & Aida, M. S. (2013). Analytical modeling and simulation of CIGS solar cells. *Energy Procedia*, *36*, 618-627.
22. Hadjab, M., Wagner, J. M., Bouzid, F., Boudour, S., Hadj Larbi, A., Bennacer, H., Ziane, Issam, M. Alam, S.M., Hamza, A. & Berrah, S. (2022). A numerical optimization study of CdS and $Mg_{0.125}Zn_{0.875}O$ buffer layers in CIGS-based solar cells using wxAMPS-1D package. *International Journal of Modelling and Simulation*, *42*(2), 179-191.
23. Moustafa, M., Al Zoubi, T., & Yasin, S. (2022). Optoelectronics Simulation of CIGS-Based Solar Cells Using a Cd-Free Nontoxic ZrS_xSe_{2-x} as a Novel Buffer Layer. *Brazilian Journal of Physics*, *52*(4), 141.
24. A. Kumar Patel, R. Mishra and S. Kumar Soni, 2023. Electrical and optical parameters optimization and interface engineering for efficiency improvement of double CIGS absorber based solar cell. Solar Energy **257**: 125-136.
25. Ranade, P., Takeuchi, H., King, T. J., & Hu, C. (2001). Work function engineering of molybdenum gate electrodes by nitrogen implantation. *Electrochemical and Solid-State Letters*, *4*(11), G85.
26. Sze, S. M., Li, Y., & Ng, K. K. (2021). *Physics of semiconductor devices*. John Wiley & Sons.
27. Gharibshahian, I., Sharbati, S., & Orouji, A. A. (2018). Potential efficiency improvement of Cu(In,Ga)Se_2 thin-film solar cells by the window layer optimization. *Thin Solid Films*, *655*, 95-104.
28. Kaufmann, C. A., Caballero, R., Unold, T., Hesse, R., Klenk, R., Schorr, S., Nichterwitz, M.& Schock, H. W. (2009). Depth profiling of Cu(In, Ga)Se_2 thin films grown at low temperatures. *Solar Energy Materials and Solar Cells*, *93*(6-7), 859-863.
29. Jackson, P., Hariskos, D., Lotter, E., Paetel, S., Wuerz, R., Menner, R., Wischmann, W. & Powalla, M. (2011). New world record efficiency for Cu(In,Ga)Se_2 thin film solar cells beyond 20%. *Progress in Photovoltaics: Research and Applications*, *19*(7), 894-897.
30. Perkins, C. L., Egaas, B., Repins, I., & To, B. (2010). Quantitative analysis of graded Cu (In_{1-x},Ga_x)Se_2 thin films by AES, ICP-OES, and EPMA. *Applied Surface Science*, *257*(3), 878-886.

31. Klenk, R. (2001). Characterisation and modelling of chalcopyrite solar cells. *Thin Solid Films*, *387*(1-2), 135-140.
32. Guillén, C., & Herrero, J. (2012). Components distribution in $Cu(In,Ga)Se_2$ films prepared by selenization of evaporated metallic precursors on bare and ITO-coated glass substrates. *Journal of Materials Science*, *47*, 1836-1842.
33. Belghachi, A., & Limam, N. (2017). Effect of the absorber layer band-gap on CIGS solar cell. Chinese Journal of Physics, 55(4), 1127-1134.
34. Jo, H. J., Kim, D. H., Kim, C., Hwang, D. K., Sung, S. J., Kim, J. H., & Bae, I. H. (2012). The optical and structural properties of CuIn1−xGaxSe2 thin films fabricated with various Ga contents by using the co-evaporation technique. Journal of the Korean Physical Society, 60, 1708-1712.
35. Moustafa, M., Al Zoubi, T., & Yasin, S. (2022). Exploration of CZTS-based solar using the ZrS2 as a novel buffer layer by SCAPS simulation. Optical Materials, 124, 112001.

A. Nassour, M. Kandouci, Z. Abu Waar, A. Belghachi, M. Moustafa. (2025). Numerical Optimization of CIGS/CGS Double-Absorber Solar Cells: Enhancing Efficiency Through Thickness and Bandgap Tuning**.** *Ukrainian Journal of Physical Optics*, *26*(2), 02104 – 02118.
doi: 10.3116/16091833/Ukr.J.Phys.Opt.2025.02104

Анотація*. У цьому дослідженні ми використали моделювання SCAPS для оцінки продуктивності інноваційної архітектури сонячного елемента на основі мідь-індій-галій-селеніду (CIGS), ретельно розробленої для досягнення вищого коефіцієнта перетворення енергії. Була застосована нова функціональність для прогнозування ширини забороненої зони та спорідненості до електронів у шарі поглинача при різних концентраціях галію (Ga) (x). Щоб зменшити рекомбінаційні втрати на задньому контакті, ми дослідили використання шару мідь-галій-селеніду (CGS) із широкою забороненою зоною (1.7 еВ) поблизу молібденового (Mo) контакту, який діє як електронний відбивач. Було продемонстровано покращення продуктивності CIGS-сонячних елементів завдяки градієнтному розподілу галію в шарі поглинача.Наші результати показали, що в конфігурації з двома шарами поглинача ефективність перетворення стабільно зростала при збільшенні товщини CGS-шару до приблизно 90% від загальної товщини поглинача. Крім того, ми дослідили вплив градієнтної зміни ширини забороненої зони в напрямку до задньої частини верхнього поглинаючого шару (тобто CIGS).Отримані результати продемонстрували, що оптимізована система CIGS (з градієнтною шириною забороненої зони)/CGS/Mo забезпечує високу фотоелектричну продуктивність, досягаючи оптимальної ефективності 25,98%.*

Ключові слова*: сонячні елементи CIGS, градієнтна заборонена зона, ефективністьперетворення, SCAPSмоделювання*